

# Temporal Shuffling for Defending Deep Action Recognition Models against Adversarial Attacks

Jaehui Hwang<sup>1</sup>, Huan Zhang<sup>2</sup>, Jun-Ho Choi<sup>1</sup>, Cho-Jui Hsieh<sup>3</sup>, and Jong-Seok Lee<sup>1</sup>

<sup>1</sup> School of Integrated Technology, Yonsei University, Korea

<sup>2</sup> Department of Computer Science, Carnegie Mellon University, PA

<sup>3</sup> Department of Computer Science, University of California, Los Angeles, CA

{jaehui.hwang, idearibosome, jong-seok.lee}@yonsei.ac.kr

huan@huan-zhang.com chohsieh@cs.ucla.edu

## Abstract

Recently, video-based action recognition methods using convolutional neural networks (CNNs) achieve remarkable recognition performance. However, there is still lack of understanding about the generalization mechanism of action recognition models. In this paper, we suggest that action recognition models rely on the motion information less than expected, and thus they are robust to randomization of frame orders. Based on this observation, we develop a novel defense method using temporal shuffling of input videos against adversarial attacks for action recognition models. Another observation enabling our defense method is that adversarial perturbations on videos are sensitive to temporal destruction. To the best of our knowledge, this is the first attempt to design a defense method specific to video-based action recognition models.

## 1. Introduction

Human action recognition has been extensively researched in recent years with the improvement of deep neural networks. A key issue in action recognition is how to effectively model the temporal motion patterns of human actions with deep models. 3D convolutional neural networks (CNNs) performing three-dimensional (2D spatial and temporal) convolutional operations are the state-of-the-art approaches for this, which achieved high recognition performance [7, 12, 13, 18, 27, 28, 28, 30].

Deep learning models have shown remarkable performance in various areas. To understand this success, researchers have explored which features the models learn and how the models generalize to unseen data, especially for object recognition in images [3, 14, 26, 29, 32, 35]. Contrary to our expectation, it was found that trained object recogni-

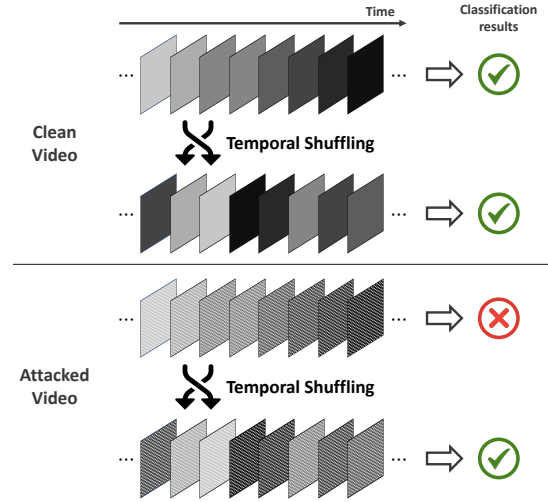


Figure 1. Illustration of the influence of temporal shuffling. Temporal shuffling is not critical to the clean original video, but destroys adversarial perturbations attacking the action recognition model. We suggest a new defense method using this property.

tion models heavily rely on components that humans hardly exploit, such as high-frequency components [29] and backgrounds [32, 35].

Motivated by these findings and considering the aforementioned key issue of action recognition models, we pose the following question: *Do trained action recognition models generalize by fully utilizing the motion pattern appearing in the input video?* In order to answer this question, we analyze the dependence of action recognition models on spatial information and temporal information for decision through various experiments. We find that the models depend on the motion information only slightly. Even when the order of video frames is randomized and the temporal information is destroyed, the models maintain relatively high recognition accuracy.

We exploit this property to propose a novel method to defend against adversarial attacks on action recognition models. In particular, we show that unlike videos, adversarial perturbations on action recognition models are easily neutralized by randomization of the frame order, which facilitates our defense method together with the aforementioned property (Figure 1).

The main contributions of this work can be summarized as follows.

- We discover that different from our expectation, state-of-the-art action recognition models rely on motion information only marginally, because they significantly depend on spatial information such as objects and backgrounds. In addition, we show that the models generalize well for varying motion speed. These characteristics make the models robust to temporal destruction such as randomization of the frame order.
- We explore the importance of temporal orders of adversarial perturbations that attack action recognition models, and find that the perturbations are sensitive to temporal destruction. Two factors behind this observation are identified, namely, the importance of the temporal pattern appearing in an adversarial perturbation and the importance of the proper temporal location of a frame perturbation.
- Based on these findings, we suggest a novel defense method, called temporal shuffling, on action recognition models. To the best of our knowledge, it is the first attempt of adversarial defense specifically targeting action recognition models.

## 2. Related work

### 2.1. Action recognition

Action recognition models have been widely researched thanks to the advances in deep neural networks. Early studies often used recurrent neural networks to model sequential features of videos [10]. However, the current state-of-the-art approach is to use 3D CNNs that can extract features considering both spatial and temporal dimensions. I3D [30] inflates 2D convolutional kernels in ResNet to 3D. In the interaction-reduced channel separated network (ir-CSN) [28], a kernel factorization technique is used to reduce computational complexity. The SlowFast network [13] is composed of two streams of 3D CNNs receiving two types of video data with different temporal resolutions. X3D [12] is based on the fast pathway of SlowFast but reduces complexity by finding optimal design factors such as temporal activation size, spatial resolution, etc.

### 2.2. Model generalization

There exist attempts to explain the remarkable generalization capability of deep neural networks for object recognition. CNNs generalize various correlations between images and their class labels [3, 14, 26, 29, 32, 35]. However, some of the correlations are different from human expectations. For instance, people hardly find meaningful information from high frequency components in images, but CNN models tend to rely on them [29]. In addition, many models exploit backgrounds of images for classification [32, 35]. However, analysis on the generalization capability of video-based action recognition models is rarely found in literature. Since video data have the temporal dimension unlike images, the findings in object recognition are not directly applied to action recognition. We present our results on this topic, particularly focusing on the temporal dimension.

### 2.3. Adversarial attack and defense

Adversarial attacks fool classification models by adding imperceptible perturbations to input data. Many deep models have shown severe vulnerability against adversarial attacks. A popular approach to attack classification models is gradient-based optimization of perturbations. The fast gradient sign method (FGSM), for instance, obtains an adversarial perturbation from the sign of the gradient of the classification loss function [15]. Its iterative version, I-FGSM [22], is widely used as a strong attack method. There exist a few attack methods on action recognition models. The sparse attack [31] aims to perturb only a few frames to attack LSTM-based models. The flickering attack [24] changes the overall color of each frame. The one frame attack [17] inserts a perturbation to only one frame by exploiting the structural vulnerability of the given model.

Several methods to defend adversarial attacks have been developed for object recognition. Heuristic approaches include random resizing [33], JPEG compression [11], bit depth reduction [34], etc. However, these tend to fail against powerful attacks. Recently, defense methods that can theoretically certify robustness have been studied. Randomized smoothing [8] adds random noise to images. Denoised smoothing [25] removes noise from attacked images.

However, there is a lack of attempts to develop defense methods for action recognition models. To our best knowledge, the proposed method in this paper is the first to defend action recognition models against adversarial attacks.

## 3. Influence of temporal changes of videos

In this section, we investigate how important temporal motion cues contained in videos are for action recognition. We first show that action recognition models are robust to destruction of temporal information. Then, experiments to explain such robustness are conducted.

Model	I3D [30]	SlowFast [13]	ir-CSN [28]	X3D [12]
Accuracy	69.1%	69.4%	62.3%	67.4%

Table 1. Classification accuracy of uniformized videos.

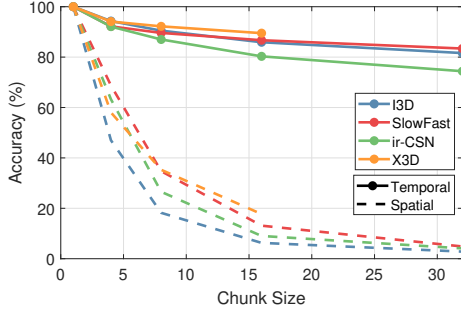


Figure 2. Classification accuracy of the videos with randomizing the order of frames with respect to the chunk size. Results with randomizing the order of rows are also shown for comparison.

### 3.1. Robustness to temporal destruction

To properly evaluate the robustness of action recognition models against the destruction of temporal information, we examine the recognition performance when the temporal information of input videos is destroyed. Two types of destruction are considered: uniformization of video frames and randomization of frame orders. The former completely removes temporal cues in a video, while the latter disturbs natural motion.

**Uniformizing video frames.** Let  $X = \{x(1), x(2), \dots, x(T)\}$  denote an original video having  $T$  frames. Then, its uniformized version is defined as  $X' = \{x(i), x(i), \dots, x(i)\}$ , where  $i \in [1, \dots, T]$ . In other words, the uniformized video is visually static without any motion. In the experiments, we try all possible values of  $i$  (i.e.,  $i=1$  to  $i=T$ ).

**Randomizing frame orders.** In this case, the frames in a video are randomly permuted. To control the amount of destruction, random permutation occurs only within each chunk composed of  $N$  frames. To be more specific, the given video is divided into multiple disjoint chunks with  $N$  successive frames, and the frame order in each chunk is randomized independently. For instance, with  $N=4$ , the first chunk can be changed from  $\{x(1), x(2), x(3), x(4)\}$  to  $\{x(3), x(1), x(4), x(2)\}$ . For comparison, spatial destruction is also conducted in a similar way, i.e., the order of the rows in each group of  $N$  rows is randomly permuted. Note that the random order is kept the same for all frames.

**Experimental details.** Kinetics-400 [20] is a popular large-scale dataset in action recognition. We randomly choose ten videos for each class from the test set of Kinetics-400. Among them, we use the 1900 videos that are correctly classified by all models for fair comparison across different models. We employ four state-of-the-art action

recognition models, including I3D [30], SlowFast [13], ir-CSN [28], and X3D [12]. We use the pre-trained models on Kinetics-400 from MMAAction2 [9]. Among the multiple versions of SlowFast and X3D, we choose  $8 \times 8$  SlowFast and X3D-M, respectively. These video dataset and models are used throughout this paper. Note that X3D receives videos having 16 frames, while 32 frames are used for the others. Thus, the chunk size for randomization is set to  $N \in \{4, 8, 16\}$  for X3D and  $N \in \{4, 8, 16, 32\}$  for the other models.

**Results.** Table 1 shows the accuracy for the uniformized videos. Note that the accuracy for the original videos is 100%. Over 60% of the uniformized videos are classified correctly by all models even though there are no motion cues in the videos. This suggests that the models can extract useful features from spatial cues.

Figure 2 shows the results for randomization of frame orders. Note that the case with  $N=1$  is for the original videos, for which the accuracy is 100%. As the chunk size becomes larger, the motion information is more distorted and thus the accuracy decreases. However, the accuracy drops are rather mild; even when the randomization is performed over the whole range (i.e.,  $N=16$  for X3D and 32 for the other models), the accuracy is higher than that for uniformized videos. Furthermore, the temporal changes degrade the recognition performance much less than the spatial changes. These results indicate that the action recognition models are robust to temporal changes. In the following, we explore reasons of this robustness further.

### 3.2. Dependence on spatial information

First, we explain the robustness of the models against temporal destruction in the viewpoint of dependence of the models on spatial and temporal information.

**Representative cases.** We distinguish the videos into three categories: (1) videos containing informative backgrounds, moving objects (whole bodies, hands, etc.), and their motion, (2) videos containing informative cues in objects and motion (but not in backgrounds), and (3) videos containing informative cues only in motion. Here, being informative means providing useful information for classification. The left panel of Figure 3 shows a representative video in each category. In Figure 3(a), there is clear information on the background (horse-breeding farm) and objects (horse and rider), which are relevant to the true class label, “Riding or walking with a horse.” Figure 3(b) with a true class label “Getting a tattoo” contains class-relevant information on the object (tattoo machine). In the third case in Figure 3(c), both background (wooden wall) and object (hand) are not so specific to the class label “Eating chips.” On the right panel of Figure 3, the accuracy of the three videos over 100 random permutations of frame orders is shown. Since the first video has rich

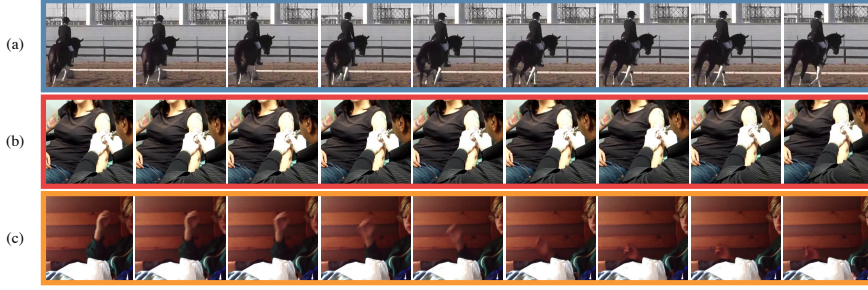


Figure 3. (Left) Example videos having different amounts of class-relevant spatial cues. (Right) Classification accuracy of the three videos under randomization of frame orders.

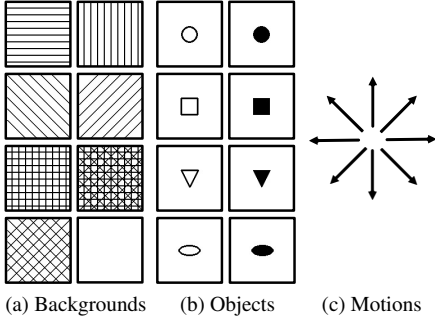


Figure 4. Patterns of backgrounds, objects, and motions used to generate datasets for the toy experiment.

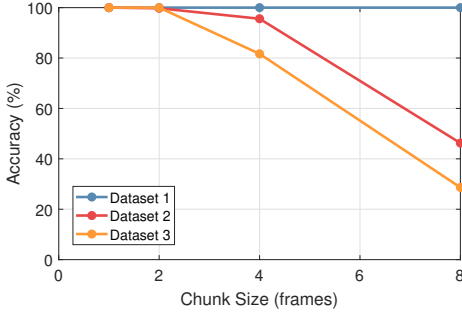


Figure 5. Classification accuracy for the toy experiment under randomization of frame orders.

spatial information, it is always correctly classified under the randomization. The second video shows moderately robust performance thanks to the class information in the object. On the other hand, the third video, which has little class-related spatial information, is vulnerable to temporal destruction. These results explain the unexpectedly high accuracy shown in Table 1 and Figure 2. The models heavily rely on spatial cues whenever available, thus the effect of temporal destruction is not significant.

**Toy experiment.** We verify the above explanation further in a controlled manner through a toy experiment. We generate three toy datasets containing videos of eight frames for eight-class problems by combining eight types of background, eight types of object, and eight motion directions, as shown in Figure 4. (1) A combination of one type of

background, one type of object, and one motion direction is assigned to each class, so that each of the background, object, and motion in a video contains class-relevant information. (2) A combination of one type of object and one motion direction is assigned to each class, while the background is randomly chosen. (3) Each class corresponds to one of the eight motion directions, and the background and object are chosen randomly. The motion speed is constant in each video between 3 and 5 pixels per frame. Each dataset contains 1600 videos, among which 75% is used for training and the rest for test. For each dataset, we train a 3D CNN model based on ResNet18 using the Adam algorithm [21], where the  $3 \times 3$  convolutional layers are inflated to  $3 \times 3 \times 3$  convolutional layers. Figure 5 shows the accuracy for the three datasets under randomization of frame orders. When spatial cues in videos are related to the class labels, the models show robust recognition performance. These results also support that the models are trained to exploit spatial cues effectively, so they become robust to temporal destruction.

### 3.3. Robustness to motion variation

We note that in Figure 5, the accuracy at  $N=8$  (i.e., randomization over all frames) for dataset 3 (with no spatial cues) is 28.7%, which is still significantly higher than random chance ( $1/8=12.5\%$ ). This suggests that even under complete randomization, certain motion cues useful for recognition still remain.

We hypothesize that *monotonicity* of motion can be informative for recognition even under temporal randomization. The second row in Figure 6 shows a part of the original video (the first row), which locally preserves the motion information. The third row, where frames are chosen at an irregular interval, contains corrupted motion but the monotonicity (i.e., the horse walking from left to right) is maintained. Randomization of frame orders may produce this type of irregular but monotonic frame orders, from which a recognition model may be able to extract useful motion features.

For the randomized frame orders obtained in Section 3.1, we calculate the ratio of monotonic frame orders in the viewpoint of the first convolutional layer of a model. For



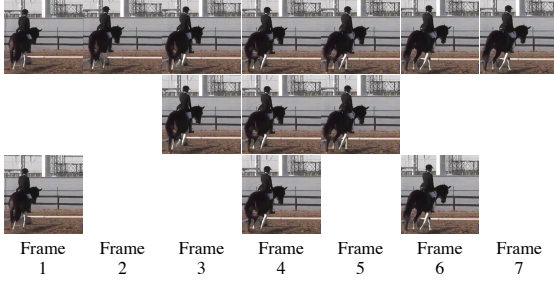


Figure 6. (Top) Original video frames. (Middle) Frames are selected consecutively. Motion information within these frames remains the same to that in the original video. (Bottom) Frames are selected irregularly. The original motion information is partly corrupted but the monotonicity is preserved.

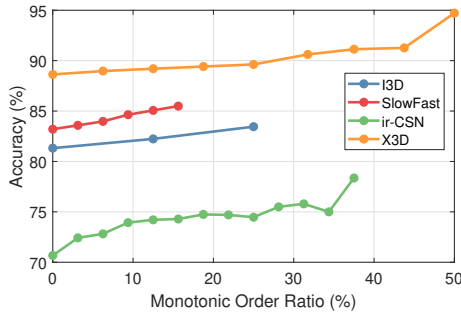


Figure 7. Classification accuracy under randomization of frame orders with respect to the ratio of monotonic orders in the viewpoint of the first convolutional layer.

example, consider a randomized order [2, 3, 4, 1, 5]. When the first convolutional layer has a temporal kernel size of 3 with a stride of 1 and zero-padding is used, the kernel processes the following five sets of frames: [2, 3], [2, 3, 4], [3, 4, 1], [4, 1, 5], and [1, 5]. Since the first, second, and the last sets contain monotonic orders, the ratio of monotonic frame orders is calculated as  $3/5=60\%$ . Figure 7 shows the recognition accuracy for the randomized videos with respect to each ratio of monotonic frame orders when  $N=32$ . Note that the possible values of the ratio are different for each model because of different kernel sizes and strides in the first convolutional layers across the models. And, the ratio values containing too few videos are excluded here. From the figure, it is observed that the accuracy increases as the ratio increases, which supports our hypothesis.

#### 4. Influence of temporal changes of adversarial perturbations

In this section, we examine the effect of temporal changes on adversarial perturbations that are added to original videos to cause misclassification. We show that unlike the clean videos (Section 3.1), adversarial perturbations are sensitive to temporal changes, and investigate reasons of such sensitivity.

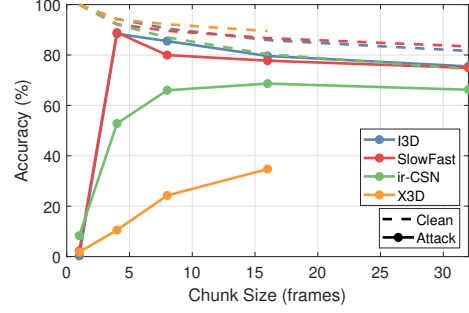


Figure 8. Classification accuracy of the attacked videos by I-FGSM ( $\epsilon=4/255$ ) after randomization of the orders of frames.

#### 4.1. Impact of temporal destruction

We use I-FGSM [22] to obtain a 3D perturbation having the same size to the given video, which is one of the widely used strong attack method, to attack videos. Let  $P^0 = \{p^0(1), p^0(2), \dots, p^0(T)\}$  denote an initial perturbation whose elements are set to zero. The attack aims to find a perturbation  $P^M$  iteratively (with  $M$  iterations), where the perturbed video by adding  $P^M$  to an original video is misclassified. In other words,  $f(X + P^M) \neq y$  while  $f(X) = y$ , where  $f(\cdot)$  is the target action recognition model. The I-FGSM update rule is applied to find  $P^{m+1}$  from  $P^m$  iteratively:

$$\tilde{P}^{m+1} = \text{Clip}_{-X, 255-X} \left( P^m + \frac{\epsilon}{M} \text{sgn}(\nabla J(X + P^m, y)) \right), \quad (1)$$

$$P^{m+1} = \text{Clip}_{-\epsilon, \epsilon}(\tilde{P}^{m+1}) \quad (2)$$

where  $\epsilon$  is the  $L_\infty$ -bound of the perturbation,  $\text{sgn}(\cdot)$  is the sign function,  $\nabla J(A, y)$  is the gradient of the loss function  $J(A, y)$ , and  $\text{Clip}_{c,d}(B) = \min(\max(B, c), d)$ , which operates as an element-wise function if  $c$  and  $d$  are matrices having the same dimension as  $B$ . After attacking the videos used in Section 3.1 by I-FGSM with  $M = 30$ , we randomize the orders of frames of the videos.

Figure 8 shows the accuracy of the attacked videos under randomization of frame orders. Without randomization ( $N=1$ ), the attack successfully fools the models, yielding accuracies of 0.3%, 2.3%, 8.3%, and 1.8% for I3D, SlowFast, ir-CSN, and X3D, respectively (the case for  $N = 1$ ). However, the temporal changes by randomization significantly reduce the effect of the attack. Except for X3D, the accuracies obtained by the three models are over 50% for all values of  $N$ . In particular, the attack is almost completely neutralized for I3D and SlowFast, achieving the accuracies close to those for the randomized clean videos.

We explore why temporal destruction can destroy adversarial attacks. In Section 4.2, we examine the importance of the temporal patterns in adversarial perturbations. Then, in Section 4.3, we show that the frame locations of adversarial perturbations are important.

	Default	Case 1	Case 2
I3D [30]	0.3%	17.9%	1.0%
SlowFast [13]	2.3%	27.5%	5.7%
ir-CSN [28]	8.3%	26.6%	11.8%
X3D [12]	1.8%	8.3%	2.4%

Table 2. Classification accuracy of the videos that are perturbed by different attack methods. ‘Default’ means the regular I-FGSM ( $\epsilon=4/255$ ), ‘Case 1’ means static perturbations, and ‘Case 2’ means perturbations generated without considering the temporal dimension.

## 4.2. Importance of temporal patterns

To study the importance of the temporal patterns of adversarial perturbations, we test the efficacy of adversarial perturbations ignoring temporal patterns in two ways. First, we set a constraint that adversarial perturbations are static over frames to exclude any temporal pattern completely. Second, we generate adversarial perturbations without considering the temporal dimension, which still vary over frames but are not optimized in the temporal dimension.

**Case 1: Generating static perturbations.** We limit a perturbation to be static, i.e.,  $P = \{p, p, \dots, p\}$ , which is found by I-FGSM. Thus, the same perturbation is added to each frame of  $X$ , so any temporal pattern does not exist in the perturbation.

**Case 2: Generating perturbations without considering the temporal dimension** In this case, we first generate one frame perturbation  $p(i)$  ( $i \in [1, \dots, T]$ ) using the method in [17] for each frame separately, and then merge them to compose  $P = \{p(1), p(2), \dots, p(T)\}$ . In this way, the perturbation does not consider the temporal dimension.

**Results.** Table 2 shows the accuracy for the two cases. Case 1 and Case 2 always yield higher accuracy (i.e., lower attack success rates) than the regular I-FGSM optimized in both spatial and temporal dimensions. Case 2, where frame-wise perturbations are generated and merged, shows lower accuracy than Case 1, which is due to higher degrees of freedom in optimizing the perturbations. These results demonstrate that temporal patterns of adversarial perturbations are important for successful attacks. Nevertheless, there exist some gaps between significant removal of the effect of attacks in Figure 8 and partial reduction of the effect of attacks in Table 2, suggesting that importance of temporal patterns is not a complete explanation for the sensitivity of adversarial perturbations to temporal destruction.

## 4.3. Importance of temporal locations

We argue that in addition to temporal patterns of adversarial perturbations, the temporal locations of the perturbations are also important for successful attacks. As a way to check this, we uniformize the attacked videos and obtain the recognition accuracy. In this case, the perturbation in each frame of the uniformized video matches the spatial content

	I3D [30]	SlowFast [13]	ir-CSN [28]	X3D [12]
Attacked	0.3%	2.3%	8.3%	1.8%
Attacked & uniformized	61.1%	60.4%	52.9%	45.9%

Table 3. Classification accuracy of the attacked videos by I-FGSM ( $\epsilon=4/255$ ) and their uniformized versions.

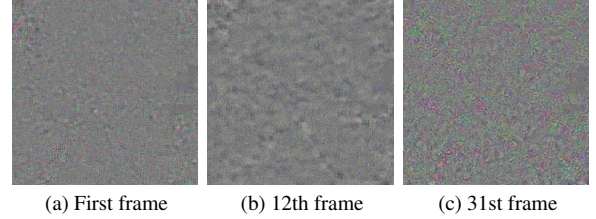


Figure 9. Adversarial perturbations on different frame locations. Magnification by  $\times 20$  is applied for visualization.

in the frame, but is placed in the  $T - 1$  locations that are different from its original temporal location. Table 3 compares the accuracy of this case with that before uniformization (i.e., videos that are only attacked). The uniformization process largely neutralizes the effect of the attack, yielding the accuracies quite close to those of the uniformized clean videos (Table 1). Therefore, a perturbation at a frame becomes ineffective when it is placed at different temporal locations.

In addition, when we generate a 3D perturbation by I-FGSM for a uniformized clean video, the perturbation at each frame location is significantly different from each other in spite of the same spatial content, as shown in Figure 9. This explains why the attacked and uniformized videos show relatively high accuracy in Table 3, and further why adversarial attacks are sensitive to temporal changes.

## 5. Temporal shuffling for defense against adversarial attacks

In Section 3, we found that the action recognition models are robust against temporal changes of input videos. On the other hand, in Section 4, we showed that adversarial perturbations do not work when the temporal orders are changed. Based on these findings, we suggest a novel defense method using temporal shuffling.

### 5.1. Method

We design our defense method based on the chunk-based randomization method in Section 3.1 with a few modifications. First, symmetric randomization of the frame order is ensured, because the chunk-based randomization is asymmetric in that the frame at the chunk boundary can be moved only in the direction keeping it within the chunk. Second, we allow a group of consecutive frames to keep their order in order to maintain the local motion pattern in the group.

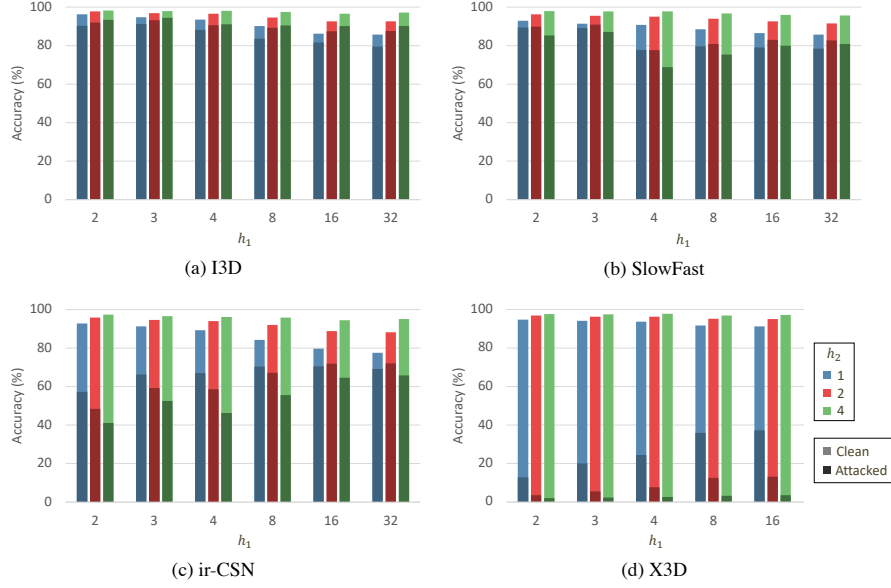


Figure 10. Classification accuracy of our defense method with various combinations of hyperparameters ( $h_1$  and  $h_2$ ). The x-axis means the value of  $h_1$ , and each color (blue, red, or green) indicates a value of  $h_2$ .

---

**Algorithm 1:** Temporal shuffling for defense

---

**input** : attacked video  $X_a$ , hyperparameters  $h_1$  and  $h_2$ , length of video  $T$   
**output** : shuffled video  $X_s$   
**initialization:**  $t \leftarrow 1$

```

1 while  $t \leq T$  do
2    $l = \max(t - h_1, 1)$ 
3    $u = \min(t + h_1, T - h_2 + 1)$ 
4   do
5      $t' \leftarrow \text{Rnd}(l, u)$   $\triangleright$  Random integer between  $l$  and  $u$ 
6     while  $t' = t$ ;
7     for  $j \leftarrow 0$  to  $h_2 - 1$  do
8        $X_s(t + j) \leftarrow X_a(t' + j)$ 
9     end
10     $t \leftarrow t + h_2$ 
11  end
12 return  $X_s$ 

```

---

Algorithm 1 shows the procedure of our defense method. First, at each frame location  $t$  of the shuffled (i.e., defended) video, we randomly choose a new frame location among  $[t - h_1, \dots, t - 1, t + 1, \dots, t + h_1]$ . Then, consecutive  $h_2$  frames starting at the chosen frame location in the given (attacked) video are copied. For instance, when  $h_1=4$  and  $h_2=3$ , the 10th frame of the shuffled video is chosen between the 6th and 14th frames of the given video; if the 14th frame is chosen randomly, the 14th to 16th frames of the given video become the 10th to 12th frames of the shuffled video.

For stability and performance, we use the ensemble technique, i.e., temporal shuffling is conducted multiple times and the final recognition result is obtained by ensembling

Ensemble size		10	20	100
I3D [30]	Clean	97.7%	97.9%	97.9%
	Attacked	94.1%	94.3%	94.4%
SlowFast [13]	Clean	95.9%	96.1%	96.2%
	Attacked	89.1%	89.6%	89.8%
ir-CSN [28]	Clean	88.1%	88.8%	88.9%
	Attacked	70.3%	71.6%	71.8%
X3D [12]	Clean	90.8%	91.1%	91.3%
	Attacked	37.6%	38.0%	37.3%

Table 4. Classification accuracy of our defense method using different ensemble sizes.

them [6, 8, 23, 25].

## 5.2. Experimental results

**Hyperparameters and ensemble size.** Figure 10 shows the accuracy of our defense method against the I-FGSM attack with  $\epsilon=4/255$  for various combinations of the hyperparameters. Here, the ensemble size is set to 100. Considering the performance for both clean videos and attacked videos, we can choose an optimal hyperparameter set as  $\{h_1, h_2\} = \{3, 4\}$  for I3D,  $\{2, 2\}$  for SlowFast,  $\{16, 2\}$  for ir-CSN, and  $\{16, 1\}$  for X3D. In [17], it was shown that ir-CSN has high transferability of adversarial perturbations between nearby frames, while I3D and SlowFast has low transferability. We additionally found that X3D also has high transferability. Thus, ir-CSN and X3D need large values of  $h_1$  to avoid shuffling among nearby frames. In the case of SlowFast, it has high transferability of perturbations between every four frame locations [17]. Thus, setting  $h_1 < 4$  is effective for defense to exclude possibility of

copying frames between transferable frame locations. If  $h_2$  is large, local motion patterns tend to be preserved. As a result, the accuracy of clean videos is kept high, but the accuracy of attacked videos remains low in many cases because the temporal patterns in the perturbations are not destroyed well. A reasonable choice of the value of  $h_2$  to balance this trade-off varies among the models.

With these optimal hyperparameter sets, Table 4 shows the classification accuracy with respect to the ensemble size. While a larger size of ensemble yields higher accuracy, the improvement is marginal. Thus, we set the ensemble size to 10 in the following comparison study.

**Comparison.** Our defense method is evaluated against several attack methods in comparison to existing defense methods. Since there is no existing defense method specifically designed for video recognition, we compare our method to two representative defense methods used in object recognition: randomized smoothing for certified robustness [8] and denoised smoothing for provable defense [25]. Furthermore, we examine the performance when our method is combined with one of them; our method destroys the temporal structure of perturbations while randomized smoothing and denoised smoothing compensate for spatial perturbations, and thus performance boosting may be expected by combining them. For attack methods, we use I-FGSM [22], flickering attack [24], one frame attack [17], and expectation over transformation (EOT) [1,2]. The flickering attack and one frame attack specifically target action recognition models. EOT, which is strong against many randomized defense methods in object recognition, works with knowledge of the existence and type of defense. It is optimized for each defense method.

Table 5 shows the comparison results. Except for a few cases of X3D, our method achieves higher accuracy than the existing defense methods. Furthermore, combining our method with the existing defense methods shows further improvement in many cases. Our method is also effective against the one frame attack. Although a perturbation created by the one frame attack does not have a temporal structure, our defense can neutralize it by changing its temporal location (Section 4.3). Our method is effective even against EOT. This is probably because there are too many possible frame order permutations that result in videos having significantly different characteristics, which is challenging for EOT to cover effectively.

## 6. Conclusion

We suggested that the action recognition models depend largely on spatial information for recognition, leading to an interesting phenomenon that the models are not influenced significantly by temporal randomization of input videos. On the other hand, we found that changing temporal orders of adversarial perturbations are fatal to successful attack.

		Clean	I-FGSM [22]	Flickering [24]	OFA [17]	EOT [1]
I3D [30]	No	100%	0.3%	29.3%	0.4%	5.5%
	RS	77.9%	44.4%	34.8%	42.5%	55.1%
	Denoise	88.3%	60.1%	36.8%	63.3%	31.1%
	Ours	<b>97.7%</b>	<b>94.1%</b>	<b>82.8%</b>	<b>97.7%</b>	<b>97.6%</b>
	Ours+RS Ours+D	<u>97.9%</u> <u>97.2%</u>	<u>94.4%</u> <u>96.2%</u>	82.4% 81.5%	97.4% 97.1%	97.4% 97.2%
Slow Fast [13]	No	100%	2.3%	36.1%	3.3%	7.9%
	RS	77.8%	45.7%	40.9%	55.5%	58.6%
	Denoise	92.2%	51.5%	46.4%	74.8%	36.4%
	Ours	<b>95.9%</b>	<b>89.1%</b>	<b>80.4%</b>	<b>95.4%</b>	<b>94.8%</b>
	Ours+RS Ours+D	<u>96.4%</u> <u>95.8%</u>	90.1% <u>90.2%</u>	80.4% <u>80.7%</u>	95.3% <u>95.7%</u>	<u>95.4%</u> 94.8%
ir-CSN [28]	No	100%	8.3%	31.9%	9.9%	13.2%
	RS	75.8%	51.7%	39.3%	51.7%	52.2%
	Denoise	<b>89.3%</b>	67.6%	40.8%	74.3%	37.4%
	Ours	88.1%	<b>70.3%</b>	<b>71.2%</b>	<b>86.5%</b>	<b>74.3%</b>
	Ours+RS Ours+D	87.2% 87.1%	76.4% <u>78.8%</u>	<u>71.6%</u> 70.2%	85.3% 86.1%	76.0% <u>77.4%</u>
X3D [12]	No	100%	1.8%	36.7%	1.7%	9.2%
	RS	80.9%	63.0%	51.6%	62.3%	58.1%
	Denoise	90.1%	<b>74.4%</b>	56.3%	<b>81.3%</b>	<b>74.4%</b>
	Ours	<b>90.8%</b>	37.6%	<b>73.3%</b>	48.3%	52.2%
	Ours+RS Ours+D	83.9% 79.3%	70.9% <u>76.1%</u>	68.3% 64.5%	73.4% 77.7%	64.3% <u>74.6%</u>

Table 5. Evaluation of our method in terms of recognition accuracy against various attack methods (I-FGSM [22], flickering attack [24], one frame attack (OFA) [17], and expectation over transformation (EOT) [1]) in comparison to existing defense methods (randomized smoothing (RS) [8] and denoised smoothing (Denoise) [25]). ‘No’ means the case without defense. ‘Ours+RS’ and ‘Ours+D’ indicate the cases where our defense is combined with the randomized smoothing and denoised smoothing, respectively. The best defense method among randomized smoothing, denoised smoothing, and ours is highlighted with bold faces for each attack method. The better method between ‘Ours+RS’ and ‘Ours+D’ is underlined when the accuracy is higher than the best defense method.

Based on these discoveries, we proposed a defense method using temporal shuffling for action recognition models. Our method achieved high defense performance under various attack and defense scenarios.

## 7. Limitation and future work

Our experiments were conducted on one of the most popular datasets, Kinetics-400. Nevertheless, it would be still necessary to perform further analysis using other datasets that may have different characteristics, e.g., sports-1M [19], which contains only sports videos, and AVA [16], which is an extensive dataset. Furthermore, we can utilize insights gained with this analysis to generate a non-biased video dataset similar to [4,5].



## References

- [1] Anish Athalye, Nicholas Carlini, and David Wagner. Obfuscated gradients give a false sense of security: Circumventing defenses to adversarial examples. In *Proceedings of the International Conference on Machine Learning*, 2018. 8
- [2] Anish Athalye, Logan Engstrom, Andrew Ilyas, and Kevin Kwok. Synthesizing robust adversarial examples. In *Proceedings of the International Conference on Machine Learning*, 2018. 8
- [3] Nicholas Baker, Hongjing Lu, Gennady Erlikhman, and Philip J Kellman. Deep convolutional networks do not classify based on global object shape. *PLoS Computational Biology*, 14(12):e1006613, 2018. 1, 2
- [4] Andrei Barbu, David Mayo, Julian Alverio, William Luo, Christopher Wang, Dan Gutfreund, Josh Tenenbaum, and Boris Katz. Objectnet: A large-scale bias-controlled dataset for pushing the limits of object recognition models. In *Proceedings of the Advances in Neural Information Processing Systems*, 2019. 8
- [5] Sara Beery, Grant Van Horn, and Pietro Perona. Recognition in terra incognita. In *Proceedings of the European Conference on Computer Vision*, 2018. 8
- [6] Xiaoyu Cao and Neil Zhenqiang Gong. Mitigating evasion attacks to deep neural networks via region-based classification. In *Proceedings of the 33rd Annual Computer Security Applications Conference*, 2017. 7
- [7] Joao Carreira and Andrew Zisserman. Quo vadis, action recognition? a new model and the kinetics dataset. In *Proceedings of the IEEE Conference on Computer Vision and Pattern Recognition*, 2017. 1
- [8] Jeremy Cohen, Elan Rosenfeld, and Zico Kolter. Certified adversarial robustness via randomized smoothing. In *Proceedings of the International Conference on Machine Learning*, 2019. 2, 7, 8
- [9] MMAAction2 Contributors. Openmmlab’s next generation video understanding toolbox and benchmark. <https://github.com/open-mmlab/mmaaction2>, 2020. 3
- [10] Jeffrey Donahue, Lisa Anne Hendricks, Sergio Guadarrama, Marcus Rohrbach, Subhashini Venugopalan, Kate Saenko, and Trevor Darrell. Long-term recurrent convolutional networks for visual recognition and description. In *Proceedings of the IEEE Conference on Computer Vision and Pattern Recognition*, 2015. 2
- [11] Gintare Karolina Dziugaite, Zoubin Ghahramani, and Daniel M. Roy. A study of the effect of JPG compression on adversarial images. *arXiv:1608.00853*, 2016. 2
- [12] Christoph Feichtenhofer. X3d: Expanding architectures for efficient video recognition. In *Proceedings of the IEEE/CVF Conference on Computer Vision and Pattern Recognition*, 2020. 1, 2, 3, 6, 7, 8
- [13] Christoph Feichtenhofer, Haoqi Fan, Jitendra Malik, and Kaiming He. Slowfast networks for video recognition. In *Proceedings of the IEEE International Conference on Computer Vision*, 2019. 1, 2, 3, 6, 7, 8
- [14] Robert Geirhos, Patricia Rubisch, Claudio Michaelis, Matthias Bethge, Felix A Wichmann, and Wieland Brendel. Imagenet-trained cnns are biased towards texture; increasing shape bias improves accuracy and robustness. In *Proceedings of the International Conference on Learning Representations*, 2019. 1, 2
- [15] Ian J Goodfellow, Jonathon Shlens, and Christian Szegedy. Explaining and harnessing adversarial examples. In *Proceedings of the International Conference on Learning Representations*, 2014. 2
- [16] Chunhui Gu, Chen Sun, David A Ross, Carl Vondrick, Caroline Pantofaru, Yeqing Li, Sudheendra Vijayanarasimhan, George Toderici, Susanna Ricco, Rahul Sukthankar, et al. Ava: A video dataset of spatio-temporally localized atomic visual actions. In *Proceedings of the IEEE Conference on Computer Vision and Pattern Recognition*, 2018. 8
- [17] Jaehui Hwang, Jun-Hyuk Kim, Jun-Ho Choi, and Jong-Seok Lee. Just one moment: Structural vulnerability of deep action recognition against one frame attack. In *Proceedings of the IEEE/CVF International Conference on Computer Vision*, 2021. 2, 6, 7, 8
- [18] Shuiwang Ji, Wei Xu, Ming Yang, and Kai Yu. 3d convolutional neural networks for human action recognition. *IEEE Transactions on Pattern Analysis and Machine Intelligence*, 35(1):221–231, 2012. 1
- [19] Andrej Karpathy, George Toderici, Sanketh Shetty, Thomas Leung, Rahul Sukthankar, and Li Fei-Fei. Large-scale video classification with convolutional neural networks. In *Proceedings of the IEEE conference on Computer Vision and Pattern Recognition*, 2014. 8
- [20] Will Kay, Joao Carreira, Karen Simonyan, Brian Zhang, Chloe Hillier, Sudheendra Vijayanarasimhan, Fabio Viola, Tim Green, Trevor Back, Paul Natsev, et al. The kinetics human action video dataset. *arXiv:1705.06950*, 2017. 3
- [21] Diederik P. Kingma and Jimmy Ba. Adam: A method for stochastic optimization. In *Proceedings of the International Conference for Learning Representations*, 2015. 4
- [22] Alexey Kurakin, Ian Goodfellow, and Samy Bengio. Adversarial examples in the physical world. In *Proceedings of the International Conference on Learning Representations Workshop*, 2017. 2, 5, 8
- [23] Xuanqing Liu, Minhao Cheng, Huan Zhang, and Cho-Jui Hsieh. Towards robust neural networks via random self-ensemble. In *Proceedings of the European Conference on Computer Vision*, 2018. 7
- [24] Roi Pony, Itay Naeh, and Shie Mannor. Over-the-air adversarial flickering attacks against video recognition networks. In *Proceedings of the IEEE/CVF Conference on Computer Vision and Pattern Recognition*, 2021. 2, 8
- [25] Hadi Salman, Mingjie Sun, Greg Yang, Ashish Kapoor, and J Zico Kolter. Denoised smoothing: A provable defense for pretrained classifiers. *Proceedings of the Advances in Neural Information Processing Systems*, 2020. 2, 7, 8
- [26] Rakshith Shetty, Bernt Schiele, and Mario Fritz. Not using the car to see the sidewalk—quantifying and controlling the effects of context in classification and segmentation. In *Proceedings of the IEEE/CVF Conference on Computer Vision and Pattern Recognition*, 2019. 1, 2
- [27] Du Tran, Lubomir Bourdev, Rob Fergus, Lorenzo Torresani, and Manohar Paluri. Learning spatiotemporal features with

- 3d convolutional networks. In *Proceedings of the IEEE International Conference on Computer Vision*, 2015. [1](#)
- [28] Du Tran, Heng Wang, Lorenzo Torresani, and Matt Feiszli. Video classification with channel-separated convolutional networks. In *Proceedings of the IEEE International Conference on Computer Vision*, 2019. [1](#), [2](#), [3](#), [6](#), [7](#), [8](#)
- [29] Haohan Wang, Xindi Wu, Zeyi Huang, and Eric P Xing. High-frequency component helps explain the generalization of convolutional neural networks. In *Proceedings of the IEEE/CVF Conference on Computer Vision and Pattern Recognition*, 2020. [1](#), [2](#)
- [30] Xiaolong Wang, Ross Girshick, Abhinav Gupta, and Kaiming He. Non-local neural networks. In *Proceedings of the IEEE Conference on Computer Vision and Pattern Recognition*, 2018. [1](#), [2](#), [3](#), [6](#), [7](#), [8](#)
- [31] Xingxing Wei, Jun Zhu, Sha Yuan, and Hang Su. Sparse adversarial perturbations for videos. In *Proceedings of the AAAI Conference on Artificial Intelligence*, 2019. [2](#)
- [32] Kai Yuanqing Xiao, Logan Engstrom, Andrew Ilyas, and Aleksander Madry. Noise or signal: The role of image backgrounds in object recognition. In *Proceedings of the International Conference on Learning Representations*, 2020. [1](#), [2](#)
- [33] Cihang Xie, Jianyu Wang, Zhishuai Zhang, Zhou Ren, and Alan Yuille. Mitigating adversarial effects through randomization. In *Proceedings of the International Conference on Learning Representations*, 2018. [2](#)
- [34] Weilin Xu, David Evans, and Yanjun Qi. Feature squeezing: Detecting adversarial examples in deep neural networks. In *Proceedings of the Annual Network and Distributed System Security Symposium*, 2018. [2](#)
- [35] Zhuotun Zhu, Lingxi Xie, and Alan L Yuille. Object recognition with and without objects. In *Proceedings of the International Joint Conference on Artificial Intelligence*, 2017. [1](#), [2](#)